

# Semi-supervised Soil Moisture Prediction through Graph Neural Networks

**Anoushka Vyas<sup>\*1</sup>, Sambaran Bandyopadhyay<sup>†2</sup>**

<sup>1</sup> International Institute of Information Technology, Hyderabad

<sup>2</sup> IBM Research AI

anoushka.vyas@students.iiit.ac.in, samb.bandyo@gmail.com

## Abstract

Recent improvement and availability of remote satellite and IoT data offers interesting and diverse applications of artificial intelligence in precision agriculture. Soil moisture is an important component of multiple agricultural and food supply chain practices. It measures the amount of water stored in various depth of soil. Existing data driven approaches for soil moisture prediction use conventional models which fail to capture the dynamic dependency of soil moisture values in near-by locations over time. In this work, we propose to convert the problem of soil moisture prediction as a semi-supervised learning on temporal graphs. We propose a dynamic graph neural network which can use the dependency of related locations over a region to predict soil moisture. However, unlike social or information networks, graph structure is not explicitly given for soil moisture prediction. Hence, we incorporate the problem of graph structure learning in the framework of dynamic GNN. Our algorithm, referred as *DGLR*, provides an end-to-end learning which can predict soil moisture over multiple locations in a region over time and also update the graph structure in between. Our solution achieves state-of-the-art results on real-world soil moisture datasets compared to existing machine learning approaches.

## 1 Introduction

Precision agriculture (Zhang, Wang, and Wang 2002) is the science of observing, assessing and controlling agricultural practices such as monitoring soil, crop and climate in a field; detection and prevention of pest and disease attacks; providing a decision support system (Baggio 2005). It can help optimizing the natural resources needed for agricultural activities and thus ensures an efficient, sustainable and environment friendly development of agriculture. Remote sensing technology (Liaghat, Balasundram et al. 2010) can be used as an effective tool in precision agriculture by providing high resolution satellite imagery with rich information about crop status, crop stresses such as nutrient and water stress, weed infestations, etc. Similarly, recent development of IoT technology (Zhao et al. 2010) can also provide useful ground truth agricultural information from local sensors and agricultural drones (Puri, Nayyar, and Raja 2017). Thus, availability of historical and real-time data has significantly

improved the scope of applying artificial intelligence for precision agricultural practices (Jha et al. 2019; Smith 2020).

In this work, we primarily focus on soil moisture, which is an important component of precision agriculture for crop health and stress management, irrigation scheduling, food quality and supply chain (Kechavarzi et al. 2010). Soil moisture measures the amount of water stored in various depth of soil. Forecasting high resolution and accurate soil moisture well ahead of time helps to save natural resources such as water and also controls the stress level of the crops. Soil moisture can be measured by soil sensors in the field (Hummel, Sudduth, and Hollinger 2001) or physics based land surface models (Rui and Beaudoin 2011). However, they have several shortcomings. Deploying soil moisture sensors on a vast region is expensive and they cannot provide forecasts. Physics based soil moisture estimation can be quite accurate, but they need extremely rich set of input features such as different soil properties, landscape information, crop information which are difficult to obtain. These physical models are also computationally heavy, making them infeasible to scale over a larger region.

There are also data driven and machine learning approaches present for soil moisture estimation. They can run with a flexible set of input features such as weather information, features derived from remote satellite imagery and are computationally fast (Dasgupta, Das, and Padmanaban 2019). However, existing approaches use conventional modeling of soil moisture using methods like support vector regression, neural networks and time series analysis. These models, though simple in nature, fail to exploit the rich spatial dependency that soil moisture values over a region exhibit. For example, if there is a rainfall, soil moisture values over the whole region increases. In an agricultural region, soil moisture values exhibits similar patterns with varying crop cycles. Conventional machine learning approaches mentioned above essentially treat different locations independently while modeling soil moisture. There exist methods in machine learning to capture such spatial dependencies through latent variable models (Castro, Paleti, and Bhat 2012), but they are complex in nature (with large number of parameters) and difficult to apply for soil moisture estimation as getting ground truth soil moisture data is expensive because of the cost of deploying physical sensors.

To address the above issues, we propose the prediction of

<sup>\*</sup>AV was an intern in IBM Research AI when the work was done

<sup>†</sup>Both the authors contributed equally

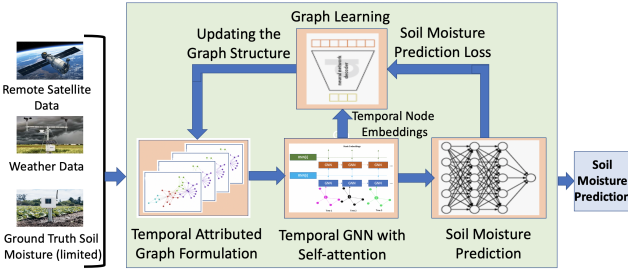


Figure 1: Solution Approach for Soil Moisture Modeling

soil moisture as a semi-supervised learning approach on dynamic graphs (also called temporal graphs) where the structure of the graph and node attributes change over time to capture the spatio-temporal variation of soil moisture. A graph can be visualized as a connected (by edges) set of entities (nodes). Intuitively, more is the correlation between the soil moisture values in two locations, more should be the chance of them to be connected in the graph. But there are challenges involved in such modeling. Unlike social networks where the graph structure is explicitly given (Karrer and Newman 2011), there is no ground truth, or even noisy graph structure given as an input for the problem of soil moisture prediction. It is possible that correlation between soil moisture values in two near-by locations are negligible due to sudden changes of soil type or landscape or other hidden factors. Thus, we also need to learn the graph structure of the problem along with the prediction of soil moisture. Recently, graph representation learning, or more specifically graph neural networks (Wu et al. 2019a) are able to achieve state-of-the-art performance on several learning tasks on graph. Our approach combines these two different domains to address the problem of soil moisture prediction. Following are the novel contributions we make in this paper:

- We pose the problem of soil moisture prediction as a semi-supervised learning problem on dynamic graphs to capture the spatio-temporal nature of soil moisture.
- As there is no graph structure given as an input to this problem, we learn and update the graph structure while modeling moisture in an end-to-end fashion.
- We propose a novel dynamic graph neural network for this purpose, which is referred as DGLR (Dynamic Graph Learning through Recurrent graph neural network). To the best of our knowledge, this solution is the first of its kind to combine dynamic graph neural networks with structure learning for applications to precision agriculture.
- We experiment on real-world soil moisture datasets to show the merit of the proposed approach, along with its different components.

## 2 Background and Related Work

We briefly cover some background on soil moisture estimation and graph representation learning, and cite existing GNNs for dynamic graphs in this section. As discussed in Section 1, conventional machine learning approaches have

been applied with diverse set of features for soil moisture estimation (Das et al. 2018). Soil moisture is directly related to weather parameters such as temperature, precipitation and relative humidity. It also depends on the agricultural use of the land. Normalized Difference Vegetation Index (NDVI) (Pettorelli 2013) is a popularly used metric to measure the greenness of a field. NDVI can also be estimated using satellite data from sources like MODIS and Sentinel-2 (D’Odorico et al. 2013). NDVI can provide useful information for soil moisture prediction. Besides, there are other sources such as soil type, landscape information and agricultural practices such as irrigation scheduling which have direct impact on moisture contained in the soil. But they are often difficult to obtain for real-life applications.

Next, the goal of graph representation learning is to obtain vector representation of different components of the graph (such as nodes) (Hamilton, Ying, and Leskovec 2017). Such vector representations can be directly fed to machine learning algorithms to facilitate graph mining tasks. There exist random walk (Perozzi, Al-Rfou, and Skiena 2014), matrix factorization (Bandyopadhyay, Lokesh, and Murty 2019) and deep neural network (Wang, Cui, and Zhu 2016) based algorithms for graph representation learning. However, graph neural networks (GNNs) are able to achieve significant attention in last few years due to their efficiency in graph representation and performance on downstream tasks. Most of the GNNs can be expressed in the form of the message passing network mentioned below (Gilmer et al. 2017):

$$h_v^l = COM^l \left( \left\{ h_v^{l-1}, AGG^k \left( \{ h_{v'}^{l-1} : v' \in \mathcal{N}_G(v) \} \right) \right\} \right).$$

Here,  $h_v^l$  is the representation of node  $v$  of graph  $G$  in  $l$ -th layer of the GNN. The function  $AGG$  (Aggregate) considers representation of the neighboring nodes of  $v$  from the  $(l-1)$ th layer of the GNN and maps them into a single vector representation. As neighbors of a node do not have any ordering in a graph and the number of neighbors can vary for different nodes,  $AGG$  function needs to be permutation invariant and should be able to handle different number of nodes as input. Then,  $COM$  (Combine) function uses the node representation of  $v$ th node from  $(l-1)$ th layer of GNN and the aggregated information from the neighbors to obtain an updated representation of the node  $v$ .

Graph neural networks are also proposed for dynamic graphs in recent years. Traffic data forecasting can naturally be posed as a prediction problem on dynamic graphs (Li et al. 2018). Temporal convolution blocks along with different types of recurrent networks are used for traffic data forecasting using GNNs (Guo et al. 2019; Yu, Yin, and Zhu 2018). Using the gated attention networks as a building block, graph gated recurrent unit is proposed to address the traffic speed forecasting problem by (Zhang et al. 2018). Traffic forecasting problem is converted to a node-wise graph and an edge-wise graph, and then a bi-component graph convolution is applied in (Chen et al. 2020). A space-time graph neural network is proposed by (Nicoliciu, Duta, and Leordeanu 2019) where both nodes and edges have dedicated neural networks for processing information. A GNN architecture, Graph WaveNet, for spatial-

Notations	Explanations
$i, j \in \{1, 2, \dots, N\} = [N]$	Indices over locations (nodes)
$d_{ij} \in \mathbb{R}_+$	Geographic distance between $i$ and $j$
$t \in \{1, 2, \dots, T\} = [T]$	Indices over time steps
$N_{tr}^t \in [N]$	Locations with soil moisture values at time $t$
$G^t = (V, E^t, X^t)$	The graph at time $t \in [T]$
$x_i^t \in \mathbb{R}^D$	Input node features for $i$ th node at time $t$
$h_i^t \in \mathbb{R}^K$	Node embedding of $i$ th node in $G^t$
$s_i^t \in \mathbb{R}$	Actual soil moisture for $i$ th station at time $t$
$\hat{s}_i^t$	Predicted soil moisture
$A^t \in \mathbb{R}^{N \times N}$	Initially constructed adjacency matrix
$\hat{A}^t = H^t H^{t \text{Trans}}$	Reconstructed adjacency matrix
$W_G$	Parameter of the GNN for the graphs
$\Theta_R = \{\Theta_{R,i} : \forall i\}$	Parameters of the RNNs for all the nodes

Table 1: Different notations used in the paper

temporal graph modeling to handle long sequences is proposed by (Wu et al. 2019b). Recurrent neural network structures that operate over a graph convolution layer to handle dynamic graphs are proposed by (Sankar et al. 2020; Pareja et al. 2020). The problem of ride-hailing demand forecasting is encoded into multiple graphs and multi-graph convolution is used in (Geng et al. 2019). However, the problem of soil moisture estimation (or similar metrics for precision agricultural applications) is quite different because of the dependency to multiple external factors and also uncertainty in the graph structure to capture spatial correlation.

### 3 Problem Formulation

We are given a set of  $N$  locations indexed by the set  $[N] = \{1, 2, \dots, N\}$  from a geographic region. There are  $[T] = \{1, 2, \dots, T\}$  time steps. For each time step  $t$ , ground truth soil moisture values are given for a subset of locations  $N_{tr}^t \subseteq [N]$ . We use  $s_i^t \in \mathbb{R}$  to denote the soil moisture at location  $i$  and time step  $t$ . For each location  $i$  and time step  $t$ , there are some  $D$  input features (such as temperature, relative humidity, precipitation, NDVI, etc.) available which might be useful to predict soil moisture. Let us denote those feature by an attribute vector  $x_i^t \in \mathbb{R}^D, \forall i \in [N], t \in [T]$ . We also assume that the geographic distance between any two locations are given. Let us use  $d_{ij}$  to denote the distance between two locations  $i$  and  $j$ . Given all these information, our goal is to predict (forecast) the soil moisture at time step  $T + 1$  for each location  $i \in [N]$ , such that the forecasting model considers both past soil moisture and input feature values, and also able to learn and exploit the relation between different locations in their soil moisture values.

In practice, retraining the model for forecasting soil moisture for every time step in future is expensive. So for our experiments in Section 5, we train (including validation) the models on the first  $\sim 80\%$  of the time interval and predict soil moisture on the rest.

### 4 Solution Approach

There are multiple stages of our integrated solution DGLR, as shown in Figure 1. We explain each of them below.

### 4.1 Initial Graph Formulation

As explained in Section 1, there is no explicit graph structure given for the problem of soil moisture prediction. To apply graph neural network in the first iteration, we use the following heuristic to form an initial graph structure. First, for each location  $i \in [N]$ , we form a node (indexed by  $i$ ) in the graph. Intuitively, if two locations are very close by, there soil moisture values can be more correlated compared to the points which are far away (there are exceptions to this and our learning algorithm is going to handle those). So, we connect any two nodes by an undirected and unweighted edge in the graph if the distance between the two corresponding locations  $d_{ij}$  is less than some pre-defined threshold. We also create a self-loop to any node in the graph. We assign attribute vector  $x_i^t \in \mathbb{R}^F$  (as discussed in Section 3) to node  $i$  at time  $t$ . According to this construction, the link structure of the graph is same across different time steps, but node features are changing. Thus, the constructed graph is dynamic in nature. Let us denote the set of graphs as  $\{G^1, \dots, G^T\}$ , where  $G^t = (V, E^t, X^t)$  is the graph<sup>1</sup> at time step  $t$  and  $V = [N]$ . We denote the adjacency matrix of  $G^t$  as  $A^t$ . We also row-normalize the adjacency matrix by dividing each row with the degree of the corresponding node.

### 4.2 Temporal Graph Neural Network

Given a dynamic graph, we develop a temporal graph neural network which can generate embedding of a node in each time step and also use that to forecast soil moisture. Each layer of the proposed temporal graph neural network has two major components. There is a self-attention based GNN (with shared parameters) similar to (Veličković et al. 2018) which works on each graph, thus capturing the spatial dependency between the nodes. The updated node embeddings from the GNN is fed to a RNN which connects graphs over different time steps to capture the temporal dependency of soil moisture. The layer is formally discussed below.

For a graph  $G^t$ , we use a trainable parameter matrix  $W$  (shared over graphs  $\forall t \in [T]$ ) to transform the initial feature vector  $x_i^t$  as  $Wx_i^t$ . As different neighboring locations may have significantly different impact on the soil moisture of a location, we use a trainable attention vector  $a \in \mathbb{R}^{2K}$  to learn the importance  $\alpha_{ij}$  for any two neighboring nodes in a graph as follows:

$$\alpha_{ij}^t = \frac{\exp\left(\text{LeakyReLU}\left(a \cdot [Wx_i^t || Wx_j^t]\right)\right)}{\sum_{j' \in \mathcal{N}_{G^t}(i)} \exp\left(\text{LeakyReLU}\left(a \cdot [Wx_i^t || Wx_{j'}^t]\right)\right)} \quad (1)$$

where  $\mathcal{N}_{G^t}(i)$  is the neighboring nodes of  $i$  (including  $i$  itself) in the graph  $G^t$ ,  $\cdot$  represents dot product between the two vectors and  $||$  is the vector concatenation. These normalized importance parameters are used to update the node features as:

$$h_i^t = \sigma\left(\sum_{j \in \mathcal{N}_{G^t}(i)} \alpha_{ij}^t A_{ij}^t Wx_j^t\right) \quad (2)$$

<sup>1</sup>Initially, the edge set is same for all the graphs, but they will change during the course of learning

where  $A_{ij}^t$  is the  $(i, j)$ th element of  $A^t$ , i.e., weight of the edge  $(i, j)$  in  $G^t$ . The sequence of updated node embeddings  $h_i^t$  of a node  $i$  over different time steps are fed to a Gated Recurrent Unit (GRU) (Chung et al. 2014), which is a popularly used recurrent neural network. The GRU unit for  $i$ th node at time step  $t$  takes the GNN output  $h_i^t$  (from Equation 2) and the GRU output  $h_i^{t-1}$  to update  $h_i^t$ , as shown below<sup>2</sup>.

$$U_i^t = \sigma(W_U^i h_i^{t-1} + P_U^i h_i^{t-1} + B_U^i) \quad (3)$$

$$R_i^t = \sigma(W_R^i h_i^t + P_R^i h_i^{t-1} + B_R^i) \quad (4)$$

$$\tilde{h}_i^t = \tanh(W_H^i h_i^t + P_H^i (R_i^t \circ h_i^{t-1}) + B_H^i) \quad (5)$$

$$h_i^t = (1 - U_i^t) \circ h_i^{t-1} + U_i^t \circ \tilde{h}_i^t \quad (6)$$

where  $U_i^t, R_i^t$  are update and reset gates of GRU at time  $t$ , respectively.  $W_U^i, W_R^i, W_H^i, P_U^i, P_R^i, P_H^i, B_U^i, B_R^i, B_H^i$  are trainable parameters of GRU for the node  $i$ . Please note that we have separate GRUs (parameters are not shared) for different nodes. This significantly help to boost the performance as the temporal trend of soil moisture values are quite different in different locations. The above completes the description of a GNN+GRU layer of our temporal graph neural network. The output of the GRU of a layer is fed as input to the next layer of GNN. Two such layers of GNN-GRU pair are used for all our experiments.

For soil moisture prediction at time  $t$ , node embeddings from the final layer GRU are used. The node embeddings from  $t-w$  to  $t-1$  are used where  $w$  is a window of time steps. We concatenate  $h_i^{t-w}, \dots, h_i^{t-1}$  and pass the vector to a fully connected layer with ReLU activation to predict the soil moisture of  $i^{th}$  node at time  $t$ , which is denoted as  $\hat{s}_i^t$ . The window  $w$  is a sliding window with stride 1. The loss of soil moisture prediction is calculated as:

$$\mathcal{L}_{STSM} = \sum_{t=w+1}^T \sum_{i \in N_{tr}^t} (s_i^t - \hat{s}_i^t)^2 \quad (7)$$

### 4.3 Updating the Graph Structure

As mentioned in Section 4.1, we use a simple heuristic to form the initial graph which may not always reflect the actual spatial dependency of soil moisture values. In this section, we try to learn the link structure between different nodes to improve the quality of the graph such that it facilitates soil moisture prediction. Recently, metrics to estimate the quality of a graph and its impact on the performance of graph neural network is shown in (Hou et al. 2020). Modifying graph structure to improve the robustness of GNN (Jin et al. 2020) and graph refinement (finding subgraph from an over-complete graph) for airway extraction (Selvan et al. 2020) are addressed in the literature. However, such solutions are often computationally expensive because of the combinatorial nature of the problem, i.e., learning edges between the nodes. Our approach is quite feasible as we learn

<sup>2</sup>We use the same notation  $h_i^t$  as the output of both GNN and GRU. But they update it sequentially.

the temporal graph structure via node embeddings as discussed below.

First, we reconstruct the adjacency matrix  $\hat{A}^t$  of the graph  $G^t$  by the similarity of the node embeddings. Formally, we obtain  $\hat{A}^t$  from the node embedding matrix  $H^t$  as:

$$\hat{A}^t = \text{ReLU}\left(H^t H^{t, \text{Trans}}\right) \in \mathbb{R}^{N \times N} \quad (8)$$

Thus,  $A_{ij}^t$  (weight of an edge) is the dot product of the two corresponding node embeddings  $h_i^t = H_{i:}^t$  and  $h_j^t = H_{j:}^t$ . The element-wise use of activation function  $\text{ReLU}(\cdot)$  ensures that reconstructed edge weights are non-negative and thus can be used in the message passing framework of GNN. Similar to  $A^t$ , we also row-normalize  $\hat{A}^t$  by degrees of the nodes. However, the reconstructed graph can be noisy if the initially obtained node embeddings are erroneous. To avoid that, we use following regularization terms.

**Graph Closeness:** Initially constructed graph with adjacency structure  $A^t, \forall t \in [T]$ , though not perfect, is easy to explain and intuitive as soil moisture values in close by regions tend to be correlated. So we want the reconstructed graph  $\hat{A}^t$  not to move very far away from  $A^t$ . To ensure that, we use the following graph closeness regularization:

$$\mathcal{L}_{GC} = \sum_{t=1}^T \text{Distance}(A^t - \hat{A}^t) \quad (9)$$

One can use any distance function between the matrices such as KL divergence or any matrix norms. We use binary cross entropy between  $A^t$  and  $\hat{A}^t$  as that produces better results.

**Feature Smoothness:** As explained in Section 1, features like weather parameters, vegetation type of the field have significant impact on soil moisture. So, locations having similar features often exhibit similar soil moisture values. It is not necessary that these locations have to be close to each other through geographic distance. Thus, we aim to connect such locations in the link structure of the graphs by using the feature smoothness regularizer as shown below:

$$\mathcal{L}_{FS} = \sum_{t=1}^T \sum_{\substack{i, j \in [N] \\ i \neq j}} \hat{A}_{ij}^t \|x_i^t - x_j^t\|^2 \quad (10)$$

Minimizing above ensures that for any time step  $t \in [T]$ , if feature vectors for two nodes  $i$  and  $j$  are similar, i.e.,  $\|x_i^t - x_j^t\|^2$  is less, the optimization would try to assign higher values to  $\hat{A}_{ij}^t$ . Similarly, if  $\|x_i^t - x_j^t\|^2$  is high for two locations  $i$  and  $j$  at time step  $t$ , feature smoothness would try to lower the weight of the edge  $(i, j)$  even if their geographic distance  $d_{ij}$  is low.

**Target Smoothness:** Finally, if two nodes have similar target variable (which is soil moisture for this work), message passing between them improves the performance of graph neural network, as observed in (Hou et al. 2020). For example in a graph dataset, if nodes which are directly connected by an edge also share same node labels, it helps the performance of node classification via message passing GNNs. As soil moisture is continuous in nature, we use the

square of the difference of two soil moisture values to find their similarity. We calculate this regularization term only on the training set  $N_{tr}^t$  for each time step  $t$ , where ground truth soil moisture is available.

$$\mathcal{L}_{TS} = \sum_{t=1}^T \sum_{\substack{i,j \in N_{tr}^t \\ i \neq j}} \hat{A}_{ij}^t (s_i^t - s_j^t)^2 \quad (11)$$

Again, minimizing target smoothness ensures that less edge weights are assigned to a node pair where nodes have very different soil moisture values. Thus, during the application of GNN, it avoids mixing features which lead to different types of soil moisture values.

#### 4.4 Joint Optimization and Training

There are multiple loss components in the overall solution of DGLR. So, we form the final loss function of DGLR by taking a linear combination of all as shown below.

$$\min_{W_G, \Theta_R} \mathcal{L}_{total} = \alpha_1 \mathcal{L}_{STSM} + \alpha_2 \mathcal{L}_{GC} + \alpha_3 \mathcal{L}_{FS} + \alpha_4 \mathcal{L}_{TS} \quad (12)$$

where  $\alpha_1, \alpha_2, \alpha_3, \alpha_4 \in \mathbb{R}_+$  are hyperparameters. In contrast to existing works which solve graph structure learning as an expensive approximation of a combinatorial optimization problem (Jin et al. 2020; Selvan et al. 2020), the variables in the optimization problem in Equation 12 are only the parameters of GNN and RNNs. Please note that we do not minimize Equations 9-11 directly with respect to the reconstructed adjacency matrix  $\hat{A}$ , rather it is always calculated as  $\hat{A}^t = \text{ReLU}(H^t H^{t \text{Trans}})$  (Equation 8) (Followed by row normalisation). Thus, instead of solving task learning (which in this case is predicting soil moisture) and graph structure learning as alternating minimization, we jointly solve both in the framework of neural networks using ADAM (Kingma and Ba 2014). Once we obtain the reconstructed adjacency matrix  $\hat{A}^t$  after optimizing Equation 12, we use  $\hat{A}^t$ , along with node feature matrices  $X^t, \forall t \in [T]$  for the next iteration of DGLR. The pseudo code of DGLR is presented in Algorithm 1. We use a simple strategy to fix the values of  $\alpha_1, \alpha_2, \alpha_3$ , and  $\alpha_4$ . We check the values of different loss components in Equation 12 and set these hyperparameters in such a way that all the components get equal weight at the beginning of the optimization.

Computation of the GNNs takes  $O(MTK)$  time, where  $M$  is the average number of edges in the initial and reconstructed graphs over time. Next, GRU takes another  $O(NTK)$  time to generate embeddings. Finally, the loss components collectively takes  $O(N^2TK)$  time. Hence, each iteration of DGLR takes  $O((N^2 + MD)TK)$  time. One can reduce the runtime of graph update regularizers by adding restriction on two nodes to get connected by an edge if their physical distance is more than some threshold, particularly for larger datasets. Besides, forming a graph across locations which are very far from each other does not make sense because of the significant change of input features, landscape, soil types, etc. Hence, DGLR can be used for real-world soil moisture prediction.

---

#### Algorithm 1 DGLR

---

**Input:** Soil moisture locations  $[N]$  and distances  $d_{ij}, \forall i, j \in [N]$  between them. Temporal attribute matrix  $X^t = \{x_i^t \mid \forall i \in [N]\}$  for each time step  $t \in [T+L]$ . Ground truth soil moisture values for (a subset of) locations from time 1,  $\dots, T$ . Window length  $w$ .

**Output:** Predict soil moisture values of all the locations from  $T+1, \dots, T+L$ .

##### Training

- 1: Construct an initial attributed graph  $G^t$  with normalized adjacency matrix  $A^t$  and node attribute matrix  $X^t$  for each time  $t \in [T]$  where each node represents one location (Section 4.1).
- 2: Set  $\tilde{A}^t = A^t, \forall t \in [T]$
- 3: **for** pre-defined number of iterations **do**
- 4:     Pass  $\tilde{A}^t$  and  $X^t$  to two layers of GNN+RNN pairs (Section 4.2) to generate all the node embeddings,  $\forall t \in [T]$ .
- 5:     Concatenate  $h_i^{t-w}, \dots, h_i^{t-1}$  and pass it to a fully connected layer to predict soil moisture  $\hat{s}_i^t, \forall i$  and  $\forall t \in \{w+1, \dots, T\}$
- 6:     Update the parameters of GNN and RNNs by minimizing the losses at Equation 12.
- 7:     Obtain  $\hat{A}^t$  by Equation 8, followed by row normalization and set  $\tilde{A}^t = \hat{A}^t, \forall t \in [T]$
- 8: **end for**

##### Soil Moisture Prediction

- 9: Pass the reconstructed graph from the last time step of training, along with attribute matrices  $X^{t-w} \dots X^{t-1}$  to the trained GNN+RNN model to predict soil moisture at time  $t, t = T+1, \dots, T+L$ .

---

## 5 Experimental Section

In this section, we discuss the details of the datasets and baseline algorithm, and analysis of the results that we obtain for soil moisture prediction.

### 5.1 Datasets Used

To the best of our knowledge, there is no publicly available benchmark dataset for spatial soil moisture prediction with the desired set of input features. So we form the following three datasets from two countries, Spain and the USA. For each dataset, we use six input features to each location for each time step. They are NDVI obtained from MODIS (<https://modis.gsfc.nasa.gov/>), SAR back scattering coefficients VV and VH from Sentinel 1 (<https://sentinel.esa.int/>), weather parameters consisting of temperature, relative humidity and precipitation (<https://www.ibm.com/weather>). Locally sensed soil moisture is collected from REMEDHUS (Sanchez et al. 2012) for Spain and from SCAN network for USA (<https://www.wcc.nrcs.usda.gov/scan/>).

**Spain:** The dataset consists of 20 soil moisture stations from North-Western Spain, for the years 2016-2017, with a temporal resolution of 15 days based on the availability of the features. It has a total of 49 time steps. We use the data from the first 40 time steps for training and validation, and last 9 time steps for testing.

**Alabama:** This dataset consists of 8 soil moisture stations from Alabama, USA during the year 2017 with a temporal resolution of 12 days and consists of 18 time steps. We use

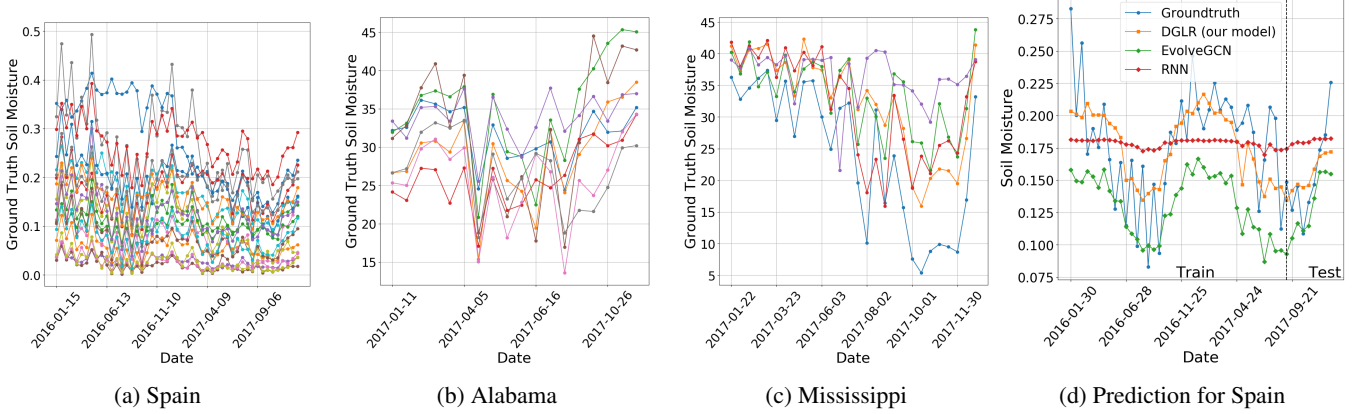


Figure 2: 2a-2c show the set of ground truth soil moisture time series from different datasets. 2d shows the actual and predicted soil moisture time series by different algorithms on a randomly selected station from the dataset Spain (best seen in color).

the first 14 time steps for training and validation, and last 4 time steps for testing.

**Mississippi:** This dataset consists of 5 soil moisture stations from Mississippi, USA during the year 2017, with a temporal resolution of roughly 10 days. We use the first 22 time steps for training and validation, and last 6 for testing.

We have plotted the ground truth soil moisture time series for each station in the three datasets in Figure 2. It can be seen that there are some similarities in the overall temporal trend of soil moisture from different stations in a dataset, but there is significant variation both in terms of their scales and fine-grained (or local) patterns.

## 5.2 Baseline Algorithms

We have used a diverse set of baseline algorithms to compare with the performance of DGLR, as follows.

**SVR and SVR-Shared** (Drucker et al. 1997): We train Support Vector Regression (SVR) to model soil moisture with respect to the features, independently for each station. For SVR-Shared, we use the same SVR model (parameters being shared) for all the stations in a dataset.

**ARIMA** (Hannan and Rissanen 1982): We use ARIMA model with Kalman filter which is widely used in time series forecasting.

**RNN and RNN-Shared** (Chung et al. 2014): A set of two RNN (GRU) layers is used on the input features for each location over time. Models are trained independently across the locations. For RNN-Shared, we train only a single GRU model (having two layers) for all the locations.

**DCRNN**(Li et al. 2018): DRCNN is a popular spatio-temporal GNN used for traffic forecasting problem. It captures the spatial dependency using bidirectional random walks on the graph, and the temporal dependency using the encoder-decoder architecture with scheduled sampling. DCRNN does not learn the graph structure. So we use it on the initially constructed graph at Section 4.1. We also use the Unicov version of DCRNN as the graph is symmetric.

**EvolveGCN**(Pareja et al. 2020): This is a recently proposed dynamic graph neural network which uses a RNN on the parameter matrices of GNN, thus captures both graph

structure and the temporal nature of the problem. Similar to DCRNN, we use EvolveGCN on the initially constructed graph in Section 4.1.

## 5.3 Model Ablation Study

There are multiple components of DGLR. In this section, we propose different variants of our model to show the usefulness of individual components of DGLR.

**DGLR (Shared):** In this variant, the parameters of the GRU are shared across all the locations in a dataset.

**DGLR (w/o SL):** Here, we train DGLR only on spatio-temporal soil moisture loss in Equation 7. In other words, we omit the graph structure learning (SL) part from DGLR.

**DGLR (w/o Sm):** In the graph update part of DGLR, we use two types of graph smoothness (Sm) regularizers (feature and target), along with the graph closeness regularizer. In this model variant, we remove feature smoothness and target smoothness components, i.e., we train DGLR with  $\alpha_3 = \alpha_4 = 0$  in Equation 12.

## 5.4 Experimental Setup

We have run all the experiments on a CPU with 2.6GHz 6-core Intel Core i7. We conduct extensive hyperparameter tuning for all the baseline algorithms and report the best results obtained. Exact values of all the hyperparameters for different algorithms on different datasets are given in the supplementary material. For DGLR and variants, we set the window length  $w = 1$  for Spain and  $w = 2$  for other two datasets. For all the GNN and deep learning based algorithms, embedding dimension  $F'$  is kept to be 10 for Spain, 8 for Alabama and 5 for Mississippi. For optimization with ADAM, learning rate is 0.0001 for Spain and 0.01 for the other two datasets, whereas we run the algorithms for 2000 epochs on Spain and 1000 epochs on the other datasets.

## 5.5 Metrics Used

We used three different metrics (Tofallis 2015) to analyze the performance of the algorithms during the test period of each time series. They are Root Mean Square Error (RMSE),

Algorithms	Spain			Alabama			Mississippi		
	RMSE (↓)	SMAPE % (↓)	Correlation (↑)	RMSE (↓)	SMAPE % (↓)	Correlation (↑)	RMSE (↓)	SMAPE % (↓)	Correlation (↑)
SVR (shared)	0.061	33.65	NA	8.51	12.68	0.143	14.07	22.28	0.368
SVR	0.052	23.84	NA	7.03	9.429	0.003	11.73	19.8	0.44
ARIMA	0.041	19	0.01	7.53	10.76	0.177	8.72	16.19	0.141
RNN (shared)	0.039	23.44	0.585	7.81	10.8	0.313	9.34	17.23	0.485
RNN	0.039	21.72	0.529	7.01	10.13	0.385	8.94	16.58	0.523
DCRNN	0.061	31.83	0.588	7.16	10.2	0.493	9.31	16.97	0.545
EvolveGCN	0.061	31.78	0.731	6.98	9.74	0.403	9.91	17.55	0.6
DGLR (shared)	0.037	17.53	0.752	6.88	9.55	0.34	8.72	15.94	0.605
DGLR (w/o SL)	0.035	15.59	0.753	5.97	8.36	0.537	8.86	16.24	0.606
DGLR (w/o Sm)	0.033	19.83	0.759	5.72	7.99	0.533	7.37	<b>12.32</b>	0.572
DGLR (our model)	<b>0.031</b>	<b>15.58</b>	<b>0.764</b>	<b>5.5</b>	<b>7.98</b>	<b>0.566</b>	<b>7.04</b>	13.2	<b>0.617</b>

Table 2: Performance of soil moisture prediction in test interval of different datasets. DGLR, as it exploits both spatial and temporal nature of the problem along with learns the graph structure, is able to perform better in most of the cases.

Missing	Spain			Alabama			Mississippi		
	SM %	RMSE (↓)	SMAPE % (↓)	Correlation (↑)	RMSE (↓)	SMAPE % (↓)	Correlation (↑)	RMSE (↓)	SMAPE % (↓)
0%	0.031	15.58	0.764	5.5	7.98	0.519	7.04	13.2	0.617
10%	0.035	18.12	0.75	5.54	7.99	0.411	9.73	17.23	0.609
20%	0.039	18.86	0.738	5.79	8.34	0.384	10.11	17.88	0.606
30%	0.039	18.96	0.661	7.13	10.51	0.627	11.02	19.11	0.605

Table 3: Test set performance of DGLR with different proportions of missing soil moisture values in the training set.

Symmetric Mean Absolute Percentage Error (SMAPE) and Correlation Coefficient. RMSE and SMAPE both measure the error in time series prediction. So lesser the value of them better is the quality. For correlation, more is the value better is the quality. RMSE is not bounded in nature, whereas SMAPE is in the range of  $[0\%, 100\%]$  and correlation is in  $[-1, +1]$ . Mathematical definitions of these metrics are included in the supplementary material.

## 5.6 Results and Analysis

We run each algorithm 10 times on each dataset and reported the average metrics over all the locations. Table 2 shows the performance of all the baselines, along with DGLR and its variants. First, we can see that algorithms with non-shared parameters across the locations in a dataset performs better than their counterparts with shared parameters. This is because soil moisture patterns in a dataset varies significantly from one location to other (Fig. 2). Next, the performance of deep sequence modeling technique like RNN is mostly better than GNN based baselines like DCRNN and EvolveGCN. This shows that using spatial information (via graph) may not always lead to a better performance, especially when the initially constructed graph is noisy. Finally, we find that DGLR is able to achieve better performance than all the baseline algorithms considered. Comparing the performance of DGLR with its variants, we can see the importance of different components of DGLR such as non-shared parameters of the GRU layers across locations, the importance of learning the graph structure and the role of feature and target smoothness regularizers. Figure 2d shows the ground truth soil moisture from a station in Spain and predicted soil moisture by DGLR and some baselines. It is quite evident that DGLR is able to match both trend and local patterns of the soil moisture, both during training and test intervals, compared to other baselines.

## 5.7 Sensitivity to Missing Soil Moisture Values

Soil moisture datasets that we use in this work do not have any missing soil moisture values. But for real-world applications, it is possible to have missing soil moisture values in between due to problem in the local sensors or in the communication networks. DGLR, being a semi-supervised approach due to use of graph neural networks, can be trained on labeled and unlabeled data points together. To see the impact of missing ground truth values in the training, we randomly remove  $p\%$  soil moisture values from the training data, where  $p \in \{10, 20, 30\}$ . Table 3 shows the test set performance of DGLR with different proportions of missing soil moisture values in the training. Please note that we still use the input features from those locations with missing soil moisture values and they do participate in the message passing framework of GNN. From Table 3, the performance of DGLR drops very slowly with more amount of missing soil moisture values in the training. In fact, its performance with 20% missing values is still better than most of the baselines in Table 2 with no missing values. So, it is clear that DGLR is quite robust in nature, and thus can be applicable for real-world soil moisture prediction.

## 6 Discussion and Conclusion

In this work, we have addressed the problem of soil moisture modeling and prediction which is of immense practical importance. We propose a semi-supervised dynamic graph neural network which also learns the graph structure over time to predict soil moisture. Our solution is robust in nature and also able to achieve state-of-the-art performance for data driven soil moisture prediction on real-world soil moisture datasets. We would also like to make our source code and datasets publicly available so that it encourages systematic development of advanced AI based approaches for soil moisture and other applications in precision agriculture.

## 7 Potential Ethical Impact and Societal Implications (Non-Technical Section)

Our work belongs to the intersection of artificial intelligence, precision agriculture and computational sustainability. Our solution is to address the real-world problem and this can help millions of farmers, agricultural practitioners and improve water resource management. However, we do not see any potential ethical issue in this work.

## References

Baggio, A. 2005. Wireless sensor networks in precision agriculture. In *ACM Workshop on Real-World Wireless Sensor Networks (REALWSN 2005), Stockholm, Sweden*, volume 20, 1567–1576.

Bandyopadhyay, S.; Lokesh, N.; and Murty, M. N. 2019. Outlier aware network embedding for attributed networks. In *Proceedings of the AAAI Conference on Artificial Intelligence*, volume 33, 12–19.

Castro, M.; Paleti, R.; and Bhat, C. R. 2012. A latent variable representation of count data models to accommodate spatial and temporal dependence: Application to predicting crash frequency at intersections. *Transportation research part B: methodological* 46(1): 253–272.

Chen, W.; Chen, L.; Xie, Y.; Cao, W.; Gao, Y.; and Feng, X. 2020. Multi-Range Attentive Bicomponent Graph Convolutional Network for Traffic Forecasting. In *The Thirty-Fourth AAAI Conference on Artificial Intelligence, AAAI 2020*, 3529–3536.

Chung, J.; Gulcehre, C.; Cho, K.; and Bengio, Y. 2014. Empirical evaluation of gated recurrent neural networks on sequence modeling. In *NIPS 2014 Workshop on Deep Learning, December 2014*.

Das, K.; Singh, J.; Hazra, J.; and Kalyanaraman, S. 2018. Evaluation of land surface model against smap and in-situ observations for indian region. In *IGARSS 2018-2018 IEEE International Geoscience and Remote Sensing Symposium*, 92–95. IEEE.

Dasgupta, K.; Das, K.; and Padmanaban, M. 2019. Soil Moisture Evaluation Using Machine Learning Techniques on Synthetic Aperture Radar (SAR) And Land Surface Model. In *IGARSS 2019-2019 IEEE International Geoscience and Remote Sensing Symposium*, 5972–5975. IEEE.

D’Odorico, P.; Gonsamo, A.; Damm, A.; and Schaeppman, M. E. 2013. Experimental evaluation of Sentinel-2 spectral response functions for NDVI time-series continuity. *IEEE Transactions on Geoscience and Remote Sensing* 51(3): 1336–1348.

Drucker, H.; Burges, C. J.; Kaufman, L.; Smola, A. J.; and Vapnik, V. 1997. Support vector regression machines. In *Advances in neural information processing systems*, 155–161.

Geng, X.; Li, Y.; Wang, L.; Zhang, L.; Yang, Q.; Ye, J.; and Liu, Y. 2019. Spatiotemporal multi-graph convolution network for ride-hailing demand forecasting. In *Proceedings of the AAAI Conference on Artificial Intelligence*, volume 33, 3656–3663.

Gilmer, J.; Schoenholz, S. S.; Riley, P. F.; Vinyals, O.; and Dahl, G. E. 2017. Neural message passing for Quantum chemistry. In *Proceedings of the 34th International Conference on Machine Learning-Volume 70*, 1263–1272.

Guo, S.; Lin, Y.; Feng, N.; Song, C.; and Wan, H. 2019. Attention based spatial-temporal graph convolutional networks for traffic flow forecasting. In *Proceedings of the AAAI Conference on Artificial Intelligence*, volume 33, 922–929.

Hamilton, W. L.; Ying, R.; and Leskovec, J. 2017. Representation learning on graphs: Methods and applications. *arXiv preprint arXiv:1709.05584*.

Hannan, E. J.; and Rissanen, J. 1982. Recursive estimation of mixed autoregressive-moving average order. *Biometrika* 69(1): 81–94.

Hou, Y.; Zhang, J.; Cheng, J.; Ma, K.; Ma, R. T. B.; Chen, H.; and Yang, M.-C. 2020. Measuring and Improving the Use of Graph Information in Graph Neural Networks. In *International Conference on Learning Representations*. URL <https://openreview.net/forum?id=rkeIIkHKvS>.

Hummel, J. W.; Sudduth, K. A.; and Hollinger, S. E. 2001. Soil moisture and organic matter prediction of surface and subsurface soils using an NIR soil sensor. *Computers and electronics in agriculture* 32(2): 149–165.

Jha, K.; Doshi, A.; Patel, P.; and Shah, M. 2019. A comprehensive review on automation in agriculture using artificial intelligence. *Artificial Intelligence in Agriculture* 2: 1–12.

Jin, W.; Ma, Y.; Liu, X.; Tang, X.; Wang, S.; and Tang, J. 2020. Graph Structure Learning for Robust Graph Neural Networks. In *Proceedings of the 26th ACM SIGKDD international conference on Knowledge discovery and data mining, KDD ’20*, 66–74. URL <https://doi.org/10.1145/3394486.3403049>.

Karrer, B.; and Newman, M. E. 2011. Stochastic blockmodels and community structure in networks. *Physical review E* 83(1): 016107.

Kechavarzi, C.; Dawson, Q.; Bartlett, M.; and Leeds-Harrison, P. 2010. The role of soil moisture, temperature and nutrient amendment on CO<sub>2</sub> efflux from agricultural peat soil microcosms. *Geoderma* 154(3-4): 203–210.

Kingma, D. P.; and Ba, J. 2014. Adam: A method for stochastic optimization. *arXiv preprint arXiv:1412.6980*.

Li, Y.; Yu, R.; Shahabi, C.; and Liu, Y. 2018. Diffusion Convolutional Recurrent Neural Network: Data-Driven Traffic Forecasting. In *International Conference on Learning Representations*.

Liaghat, S.; Balasundram, S. K.; et al. 2010. A review: The role of remote sensing in precision agriculture. *American journal of agricultural and biological sciences* 5(1): 50–55.

Nicolicioiu, A.; Duta, I.; and Leordeanu, M. 2019. Recurrent Space-time Graph Neural Networks. In *Advances in Neural Information Processing Systems*, 12838–12850.

Pareja, A.; Domeniconi, G.; Chen, J.; Ma, T.; Suzumura, T.; Kanezashi, H.; Kaler, T.; Schardl, T. B.; and Leiserson, C. E. 2020. EvolveGCN: Evolving Graph Convolutional Networks for Dynamic Graphs. In *AAAI*, 5363–5370.

Perozzi, B.; Al-Rfou, R.; and Skiena, S. 2014. Deepwalk: Online learning of social representations. In *Proceedings of the 20th ACM SIGKDD international conference on Knowledge discovery and data mining*, 701–710.

Pettorelli, N. 2013. *The normalized difference vegetation index*. Oxford University Press.

Puri, V.; Nayyar, A.; and Raja, L. 2017. Agriculture drones: A modern breakthrough in precision agriculture. *Journal of Statistics and Management Systems* 20(4): 507–518.

Rui, H.; and Beaudoin, H. 2011. Readme document for global land data assimilation system version 2 (GLDAS-2) products. *GES DISC* 2011.

Sanchez, N.; Martínez-Fernández, J.; Scaini, A.; and Perez-Gutierrez, C. 2012. Validation of the SMOS L2 soil moisture data in the REMEDHUS network (Spain). *IEEE Transactions on Geoscience and Remote Sensing* 50(5): 1602–1611.

Sankar, A.; Wu, Y.; Gou, L.; Zhang, W.; and Yang, H. 2020. DySAT: Deep Neural Representation Learning on Dynamic Graphs via Self-Attention Networks. In *Proceedings of the 13th International Conference on Web Search and Data Mining*, 519–527.

Selvan, R.; Kipf, T.; Welling, M.; Juarez, A. G.-U.; Pedersen, J. H.; Petersen, J.; and de Bruijne, M. 2020. Graph Refinement based Airway Extraction using Mean-Field Networks and Graph Neural Networks. *Medical Image Analysis* 101751.

Smith, M. J. 2020. Getting value from artificial intelligence in agriculture. *Animal Production Science* 60(1): 46–54.

Tofallis, C. 2015. A better measure of relative prediction accuracy for model selection and model estimation. *Journal of the Operational Research Society* 66(8): 1352–1362.

Veličković, P.; Cucurull, G.; Casanova, A.; Romero, A.; Liò, P.; and Bengio, Y. 2018. Graph Attention Networks. *International Conference on Learning Representations* URL <https://openreview.net/forum?id=rJXMpikCZ>.

Wang, D.; Cui, P.; and Zhu, W. 2016. Structural deep network embedding. In *Proceedings of the 22nd ACM SIGKDD international conference on Knowledge discovery and data mining*, 1225–1234.

Wu, Z.; Pan, S.; Chen, F.; Long, G.; Zhang, C.; and Yu, P. S. 2019a. A comprehensive survey on graph neural networks. *arXiv preprint arXiv:1901.00596* .

Wu, Z.; Pan, S.; Long, G.; Jiang, J.; and Zhang, C. 2019b. Graph wavenet for deep spatial-temporal graph modeling. In *Proceedings of the 28th International Joint Conference on Artificial Intelligence*, 1907–1913. AAAI Press.

Yu, B.; Yin, H.; and Zhu, Z. 2018. Spatio-temporal graph convolutional networks: a deep learning framework for traffic forecasting. In *Proceedings of the 27th International Joint Conference on Artificial Intelligence*, 3634–3640.

Zhang, J.; Shi, X.; Xie, J.; Ma, H.; King, I.; and Yeung, D. 2018. GaAN: Gated Attention Networks for Learning on Large and Spatiotemporal Graphs. In Globerson, A.; and Silva, R., eds., *Proceedings of the Thirty-Fourth Conference on Uncertainty in Artificial Intelligence, UAI 2018, Monterey, California, USA, August 6-10, 2018*, 339–349. AUAI Press. URL <http://auai.org/uai2018/proceedings/papers/139.pdf>.

Zhang, N.; Wang, M.; and Wang, N. 2002. Precision agriculture—a worldwide overview. *Computers and electronics in agriculture* 36(2-3): 113–132.

Zhao, J.-c.; Zhang, J.-f.; Feng, Y.; and Guo, J.-x. 2010. The study and application of the IOT technology in agriculture. In *2010 3rd International Conference on Computer Science and Information Technology*, volume 2, 462–465. IEEE.